Mapping of the IDDM Locus *Idd3* to a 0.35-cM Interval Containing the *Interleukin-2* Gene

Paul Denny, Christopher J. Lord, Natasha J. Hill, Juliet V. Goy, Elaine R. Levy, Patricia L. Podolin, Laurence B. Peterson, Linda S. Wicker, John A. Todd, and Paul A. Lyons

Currently, 16 loci that contribute to the development of IDDM in the NOD mouse have been mapped by linkage analysis. To fine map these loci, we used congenic mapping. Using this approach, we localized the *Idd3* locus to a 0.35-cM interval on chromosome 3 containing the *Il2* gene. Segregation analysis of the known variations within this interval indicated that only one variant, a serine-to-proline substitution at position 6 of the mature interleukin-2 (IL-2) protein, consistently segregates with IDDM in crosses between NOD and a series of nondiabetic mouse strains. These data, taken together with the immunomodulatory role of IL-2, provide circumstantial evidence in support of the hypothesis that *Idd3* is an allelic variation of the *Il2* gene, or a variant in strong linkage disequilibrium. *Diabetes* 46:695–700, 1997

Linkage analysis and congenic strain mapping have localized 16 loci (*Idd1–16*) that contribute to the development of IDDM in the NOD mouse (1,2). The presence of two loci, *Idd3* and *Idd10*, on proximal and distal chromosome 3, respectively, has been confirmed by the development of congenic strains in which chromosome regions from nondiabetic strains (e.g., B6) have been introgressed onto the NOD background (3). By mapping the boundaries of the congenic segments in these strains and measuring their diabetes frequencies, we localized *Idd3* to a 4.1-cM interval (4). A number of genes are known to lie within this interval, including a strong candidate gene that encodes the T-cell growth factor, interleukin-2 (IL-2). *Idd3* controls not only diabetes development but also the initiation and severity of T-cell infiltration and destruction of pancreatic islets (insulitis) (5–7). This result suggests that the *Idd3* protein functions in the immune system, perhaps controlling T-cell activity. However, several hundred additional, unidentified genes may also lie within this interval. Accordingly, it is essential to reduce the size of the interval to one that is amenable to the identification of all genes.

In this study, we describe the establishment of a yeast artificial chromosome (YAC) framework map of the *Idd3* region and the development of new microsatellite markers that reduce the *Idd3* interval to 0.35 cM. Analysis of known variants within this 0.35-cM interval showed that only one variant, a point mutation within exon 1 of the *Il2* gene, consistently segregated with *Idd3* in a number of different crosses involving NOD mice and nondiabetic strains.

RESEARCH DESIGN AND METHODS

Animals. We used the following congenic strains: NOD.B6^2 (N11F2-3), NOD.B6^3 (N11F2-4), and NOD.B6^7 (N13F2-3). The derivation of congenic strains NOD.B6^2 and NOD.B6^3 has been previously described (4). The congenic strain NOD.B6^7 was developed by backcrossing NOD.B6^2 to NOD and intercrossing the resulting F1 progeny. The F2 progeny were genotyped for the markers within *Idd3*, and appropriate recombinants backcrossed to NOD. F1 progeny were intercrossed to produce homozygous animals. The congenic strain was maintained by brother-sister mating. The absence of non-*Idd3* chromosomal regions that might contribute to diabetes resistance was confirmed by genotyping the founder animals of each strain using a panel of microsatellite markers that sample the entire genome (4).

PCR analysis. Sequence-tagged site (STS) polymerase chain reactions (PCRs) were performed on YAC DNA according to standard methods and analyzed on NuSieve gels (FMC Bioproducts, Rockland, ME) (8). Fluorescently labeled PCRs were performed and analyzed as described by Lord et al. (4).

Fluorescent in situ hybridization analysis. YACs were tested for chimerism by fluorescent in situ hybridization (FISH) according to the following protocol. Biotinylated YAC DNA (Bionick Labelling System, Life Technologies, Paisley, U.K.) was processed as described in Boyle et al. (9) and hybridized for 60 h to denatured metaphase spreads from mouse embryonic fibroblasts. Following hybridization, slides were washed in 50% formamide/2× saline/sodium citrate buffer for 2 × 5 min, blocked in 5% nonfat dried milk in phosphate-buffered saline (PBS)/0.1% Tween-20 for 10 min then incubated consecutively for 45 min at 37°C with goat antibiotin conjugated to fluorescein isothiocyanate (FITC; Sigma, St. Louis, MO) followed by rabbit anti-goat conjugated to FITC diluted in 5% nonfat dried milk in PBS. Incubations were followed by 3 washes in PBS/Tween. Slides were counterstained with propidium iodide in Vectorshield antifade (Vector Laboratories, Burlingame, CA) and viewed on a Nikon Optiphot (Nikon, Kingston, U.K.). Fluorescent images were visualized on a Biorad MRC 1024 Confocal microscope with Lasersharp software (BioRad Laboratories, Hemel Hempstead, U.K.).

A minimum of 10 metaphases were scored for each sample. Metaphase spreads from samples that appeared not to be chimeric were then painted with a commercial chromosome 3 mouse paint (Cambio, Cambridge, U.K.) to confirm the identity of the chromosome.

YAC manipulations. YACs were sized by pulsed-field gel analysis. Electrophoresis was performed at 200 V for 24 h at 14°C with pulse times ramped from 30 s to 120 s. Following electrophoresis, Southern blots were prepared from the gels and hybridized with ^{32}P-labeled mouse CoT-1 DNA according to

From the Wellcome Trust Centre for Human Genetics (P.D., C.J.L., N.J.H., J.V.G., J.A.T., P.A.L.), Nuffield Department of Surgery, and the Molecular Cytogenetics Unit (E.R.L.), University of Oxford, Headington, Oxford, U.K.; and the Departments of Cellular and Molecular Pharmacology (L.B.P.) and Autoimmune Diseases Research (P.L.P., L.S.W.), Merck Research Laboratories, Rahway, New Jersey.

Address correspondence and reprint requests to Dr. Paul A. Lyons, The Wellcome Trust Centre for Human Genetics, Nuffield Department of Surgery, University of Oxford, Windmill Road, Headington, OX3 7BN, U.K. E-mail: paul.lyons@well.ox.ac.uk.

Received for publication 24 May 1996 and accepted in revised form 14 November 1996.

AOD, autoimmune ovarian dysgenesis; FISH, fluorescent in situ hybridization; FITC, fluorescein isothiocyanate; IBD, identical by descent; IL-2, interleukin-2; *IL2* gene, *Interleukin-2* human gene; *Il2* gene, *Interleukin-2* rodent gene; IRE, interspersed repetitive element; NOD, nonobese diabetic; PBS, phosphate-buffered saline; PCR, polymerase chain reaction; SSLP, simple sequence length polymorphism; STS, sequence-tagged site; YAC, yeast artificial chromosome.

TABLE 1
STS content map of the *Idd3* interval

Clone	Size (kb)	FISH*	Marker: *D3Mit330*	*D3Mit167*	*D3Mit240*	*D3Mit181*	*D3Mit272*	*D3Mit168*	*D3Nds55*	*D3Mit180*	*D3Mit331*	*D3Mit223*	*D3Mit239*	*Anx-rs*	*D3Nds36 (CcnA)*	*D3Nds65*	*D3Nds64*	*D3Nds47*	*D3Nds50*	*D3Nds6 (IL2)*	*D3Nds56*	*D3Nds51*	*D3Nds34 (Fgf2)*	*D3Nds46*	*D3Nds45*	*D3Nds40*	*D3Mit169*	*D3Nds41*	*D3Nds43*	*D3Nds42*	*D3Nds44*	*D3Mit295*
mY102B6	300	C																												+	+
mY131D10	570	NC																													+
mY136H10	350	NC																													+
mY147E10	700	C																													+
mY25C9	500	NC																								+	+	+	+	+	+
mY109G9	590	NC																									+	+	+	+	+
mY162G3	780	NC																							+	+	+	+	+	+	+
mY54G3	ND	NC																			+	+	+	+	+						
mY191F6	600	C																			+	+	+	+							
mY91F12	800	NC																+	+	+	+	+	+	+	+						
mY102B12	450	NC																+	+	+	+	+	+	+							
mY146G12	680	C																		+	(–)	+	+	+							
mY184F10	1,400	C																+	+	+	+	+	+	+							
mY161C6	450	NC																+	+	+	+										
mY140A7	300	NC																	+	+	+	+									
mY78F3	580	ND												+	+	+	+														
mY102G4	ND	C												+	+	+															
mY109C12	750	C												+	+	+															
mY27D2	500	C													+	+	+														
mY34d1	ND	ND												+	+	+															
mY34e1	ND	ND												+	+	+															
mY107D3	1,200	ND											+																		
mY79C4	1,000	ND											+																		
mY132c10	ND	ND											+																		
mY86g1	ND	ND										+																			
mY166d3	ND	ND									+	+																			
mY79C7	250	ND									+	+																			
mY55f10	ND	ND						+		+																					
mY146e5	ND	ND						+		+																					
mY199c5	ND	ND						+		+																					
mY175F10	600	NC						+	+	+	+	+																			
mY168PD	ND	C				+	+	+	+																						
mY24C11	ND	NC			+																										
mY39A9	ND	ND			+																										
mY142G12	ND	ND			+																										
mY149C2	ND	NC			+	+	+																								
mY176G7	ND	NC			+	+	+																								
mY161D3	700	NC	+	+																											

C, chimeric; NC, nonchimeric; ND, not determined.

standard protocols (10). YAC insert ends were isolated by vectorette PCR as described by Riley et al. (11). Microsatellites were isolated using a method based on that described by Korn et al. (12) for the selection of transcribed sequences. Briefly, YAC vectorette libraries were amplified by interspersed repetitive element (IRE)/bubble PCR using the conditions of Munroe et al. (13). PCR products were annealed with biotinylated $(TG)_{20}$ and $(AG)_{20}$ oligonucleotides to enrich for products containing microsatellites. Following capture on streptavidin-coated magnetic beads (Dynal, Oslo, Norway), the IRE/bubble products were reamplified, cloned into pAMP10 (Life Technologies), and transformed into DH5α competent cells (Life Technologies). Clones containing microsatellites were identified by hybridizing colony lifts with ^{32}P-labeled $(TG)_8T$ and $(AG)_8A$ oligonucleotides and sequenced as previously described (4). STS and microsatellite primers were designed using the Primer software (version 0.5, available by file transfer protocol from the Whitehead Institute/MIT Center for Genome Research, Boston, MA).

Sequencing of exon 1 of the murine *Il2* gene. A 297-bp PCR fragment containing *Il2* exon 1 was amplified from genomic DNA (using the conditions described in Lord et al. [4]) with the following primers: *1*) MuIl2seqF.1, *2*) 5′-ATAAATTGCCTCCCATGCTG 3′, *3*) MuIl2seqR.1, and *4*) 5′-TTGCCTATAGATGGGATGGC-3′. Then 10 µl of the PCR product were gel purified using the

TABLE 2
Primer sequences

Marker	Type	Forward primer	Reverse primer	Product size
D3Nds40	SSLP	TCA ACA CAG ATT GAG ACT CCT G	TGG CTC ATT GGT GTG CAC	B6 = B10 > NOD = SPR
D3Nds41	SSLP	ATC CTG TAG GAA AGG CAG AGG	CAG GTT CTG TGA GCC CTT ATG	NOD = B6 = B10 > SPR
D3Nds42	SSLP	CGT TAC AAA GCA AAG CAA AGC	ACA TTA GGG TGT TGG GGA CA	SPR > B10 =B6 > NOD
D3Nds43	SSLP	ATT GTG TGT TGT TTA TGT AAG A	CAT TTT ATT TAT ACA AGC ATT T	NOD > B6 = B10 > SPR
D3Nds44	STS	GGG GAG GAA GGT AAG AGT ATC C	GGA GGG ATA CTA GCT CAC TCC C	166 bp
D3Nds45	STS	ACC AAG GCA CAA GAA ACA CC	GCA CTG TGT CCA CAT GCA G	241 bp
D3Nds46	STS	CAC CCA CAC TTA GTA CCC CTG	CAA CCC TCC AGA GAA GCA AG	117 bp
D3Nds47	STS	CCA TCT TGT TAA GAA ACC TCG G	AGT TCC TTT GAG CAG TTT CCC	168 bp
D3Nds48	SSLP	CAG GGA ATC CTG TAG GAA AGG	GGG CCC TTA TGA GCC TAA GT	NOD = B6 = B10 > SPR
D3Nds50	STS	TTG CCA CCT CTC CTG TTC TC	TCA AAA ATG AGA GAC ACA GGA A	51 bp
D3Nds51	STS	CCT TGA GGG CGA GAT AAG AA	AAA TAG CCA GCC CAC TTG G	275 bp
D3Nds55	SSLP	GAA ACC CTG TCT CAG AAA AAG A	CTT TCC GTG TCC TGC ATA GT	SPR > B10 = B6 > NOD
D3Nds56	STS	CCC CCA ACA AAG GGA GTC	GAA AGA TGA AGA TGG GAT GAT G	153 bp
D3Nds64	STS	GCC AGA ATT ACG GGG GTC	AAG CAA TTA TCG CCA ACC TG	137 bp
D3Nds65	STS	GGA AAT ATT TGC CCT GCT TC	GAT TTT CAA AAC CGC ATG TG	151 bp
*Anx-rs**	EST	AGT TCA CAA TTT CAC CGC TA	TGC TAA TGA CCA AAG GTG TC	216 bp

*Anx-rs primer sequences were provided by Dr. D. Beier, Brigham and Women's Hospital, Boston, Massachusetts. EST, expressed sequence tag; SSLP, simple sequence length polymorphism.

PCR Wizard Prep. System (Promega Biotec, Madison, WI) according to the manufacturer's instructions, and sequenced using an ABI PRISM Dye Terminator Cycle Sequencing (FS) Ready Reaction kit on a GeneAmp PCR System 9600 thermocycler (Perkin-Elmer/Cetus, Norwalk, CT). Sequence data were analyzed using Perkin-Elmer Sequencing Analysis software (Vers. 2.0.1) and assembled using the AssemblyLIGN software (Vers. 1.0.7; Eastman Kodak, Rochester, NY).

Analysis of the human *IL2* gene. Using a microsatellite marker located in the 3′ flanking region of the *IL2* gene, 284 affected sib pairs from the United Kingdom (14) were typed (15). Linkage and association analyses were performed as previously described (16). Exon 1 of the human *IL2* gene was sequenced in 87 unrelated, sporadic diabetic Caucasian patients from the U.K. and 16 nondiabetic black control subjects from Gambia (Gambian DNAs provided by Dr. A. Hill, The Wellcome Trust Centre for Human Genetics, Oxford, U.K.). A 382-bp PCR fragment containing *IL2* exon 1 was amplified from genomic DNA using a modification of the conditions described in Lord et al. (4), so that each PCR reaction contained only 0.025 mmol/l dNTPs and 31.25 ng of the following primers: *1*) Hull2seqF.1 5′-AAAACATTTTGACACCCCCA-3′ and *2*) Hull2seqR.1 5′-TCCTGGTGAGTTTGGGATTC-3′.

A second round of PCR was performed as above, using as template 5 µl of a 1/100 dilution of first-round PCR product and the following primers: *1*) Hull2seqF.2 5′-TGTAAAACGACGGCCAGTGCATCTCTTGTTCAAGAGTTC-3′ and *2*) Hull2seqR.2 5′-CAGGAAACAGCTATGACCGATCTCCAGCTAGATTAC-TAAATG-3′.

The nested PCR product was cycle sequenced (without template purification or dilution) by use of both the ABI PRISM-21M13 and M13 Reverse Dye Primer Cycle Sequencing (FS) Ready Reaction kits on a GeneAmp PCR System 9600 thermocycler (Perkin-Elmer/Cetus). Resultant extension products were purified according to the manufacturer's protocol and electrophoresed on an ABI 373 sequencer. Sequence data were analyzed using Perkin-Elmer Sequencing Analysis software (Vers. 2.0.1) and AssemblyLIGN software (Eastman Kodak).

RESULTS

Construction of a YAC framework map encompassing the *Idd3* interval. We previously localized *Idd3* to an interval of 4.1 cM between, but not including, the microsatellite markers *D3Mit167* and *D3Mit295* (4). To facilitate the isolation of new, allelically variable microsatellite markers mapping to this interval, we constructed a YAC framework map across the region (Table 1). YACs were isolated by screening the Whitehead YAC library (Research Genetics) with STSs developed in our laboratory (4) and all the available MIT microsatellites that map between *D3Mit167* and *D3Mit295* (17). In addition, an STS developed from an annexin-related sequence (*Anx-rs*) that co-maps with *D3Mit21* was used (Mouse Genome Database, Release 3.1). Following FISH analysis, the ends of the nonchimeric YACs mY78f3, -140a7, -161c6, -25c9, -162g3, -79c4, and -79c7, and the chimeric YAC mY102g4 were isolated, and those not comprising repetitive sequences were used to develop sequence-tagged sites (STSs; Table 2). Screening of our framework map with these new STS to determine overlaps between adjacent YACs indicated that the YACs fell into a total of four contiguous sequences (Table 1).

Generation of new, variant microsatellite markers and narrowing of the *Idd3* genetic interval. Six microsatellite markers, *D3Nds40–43*, *-48*, and *-55*, were isolated and characterized from the YACs mY25c9, -162g3, and -175f10, and a P1 clone (18), mP285o4 (Table 2). These markers were confirmed as mapping to the *Idd3* interval by typing recombinant panels of mice derived from the EUCIB (19) and/or the NOD × B10.$H2^{g7}$ backcrosses (5,6). Of the markers variant between the NOD and B6 strains, *D3Nds55* was mapped 1.4 cM distal to *D3Mit240* and 0.2 cM proximal to *D3Nds36* (Fig. 1); the remaining markers, *D3Nds40*, *-42*, and *-43*, were unresolved from *D3Nds36*, *-6*, and *-34*. To order these markers, they were typed on an additional 944 progeny of an F2 cross between NOD and the strain NOD.$B6^2$ (4). This gave an order of *D3Nds36*-(0.07 cM)-*D3Nds6*-(0 cM)-*D3Nds34*-(0.08 cM)-*D3Nds40*-(0.08 cM)-*D3Nds43*-(0 cM)-*D3Nds42*-(1 cM)-*D3Mit295* (Fig. 1).

Subsequent to our previous report (4), one additional microsatellite marker, *D3Mit240*, from the MIT database (17) was found to map within the *Idd3* interval and be allelically variable between the NOD and B6 strains. Typing 508 progeny of an NOD × B10.$H2^{g7}$ backcross (5,6) placed this marker with *D3Mit167*, 1.6 cM proximal to *D3Nds36* (Fig. 1).

To localize *Idd3* more precisely, we typed our *Idd3* congenic strains with these new markers (Fig. 1). Strain NOD.$B6^2$ (4) was found to be NOD derived at *D3Nds55* and

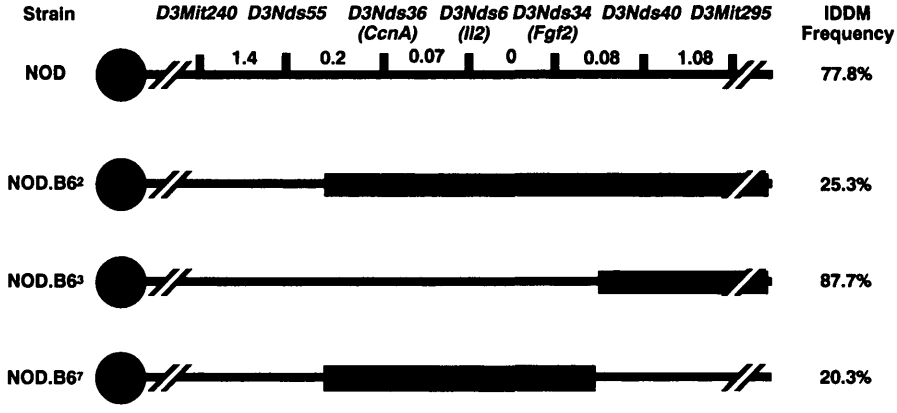

FIG. 1. High resolution genetic map of proximal chromosome 3 around *Idd3*. The lower bars show the genotypes of markers within the *Idd3* interval for the three congenic strains NOD.B6^2, NOD.B6^3, and NOD.B6^7. The solid bars indicate B6 derived genome. Distances between markers are given in centimorgans.

B6 derived at *D3Nds40*. The frequency of diabetes in females of this strain at 7 months is 25.4% (17/67) compared with 77.8% (63/81) in NOD ($P < 0.0001$), indicating that this strain carries the *Idd3* resistance allele. These results localize the proximal boundary of the *Idd3* interval between the markers *D3Mit55* and *D3Nds36*. The NOD.B6^3 strain (4) was found to be NOD derived at *D3Nds55* and B6 derived at *D3Nds40* (Fig. 1). The frequency of diabetes in females in this strain is similar to NOD at 7 months (87.7% [50/57] vs. 77.8% [63/81]; $P > 0.05$); therefore, this strain must carry the *Idd3* susceptibility allele. Thus the distal boundary of the *Idd3* interval must lie between the markers *D3Nds40* and *D3Nds34*. The mapping of the distal boundary is confirmed by the reciprocal congenic strain, NOD.B6^7, which is NOD derived at *D3Nds40* and B6 derived at *D3Nds34*. This strain has a frequency of diabetes in females at 7 months of 20.3% (12/59; $P < 0.0001$ compared with NOD), and thus must carry the resistance allele at *Idd3*. On the basis of these typings, we reduced the *Idd3* interval to 0.35 cM between, but not including, the markers *D3Nds55* and *D3Nds40* (Fig. 1).

Segregation analysis of allelic variants within the 0.35-cM *Idd3* interval. Following the localization of *Idd3* to within the *D3Nds55–D3Nds40* interval, we attempted to assess which known allelic variants within the *Idd3* region consistently segregated with the inheritance of IDDM.

To this end, we analyzed a number of inbred mouse strains according to the following parameters: *1*) the genotypes of microsatellites within and around the *Idd3* region, *2*) the predicted amino acid sequences of the allelically variable exon 1 of the *Il2* gene, and *3*) whether or not *Idd3* segregates with the inheritance of IDDM in crosses between NOD and the diabetes-resistant strain in question (Table 3).

In crosses where segregation at *Idd3* is observed, loci that are allelically identical between NOD and the diabetes-resistant strain are less likely to be candidates for *Idd3*. Thus *D3Nds55* and *D3Mit239* are unlikely candidates because the NON strain, which shows segregation at *Idd3* in crosses with NOD and is assumed to possess the diabetes and insulitis resistance allele at *Idd3*, possesses the NOD allele at both loci (Table 3). Conversely, in crosses where segregation at *Idd3* is not observed, loci that are variant are also less likely to be *Idd3*. Thus the loci *D3Nds55*, *D3Nds239*, *D3Nds36*, *D3Nds6*, *D3Nds34*, and *D3Nds40* are unlikely to be *Idd3* because the PWK, SWR, and SEG strains, which show no segregation at *Idd3* and are assumed to possess the *Idd3* susceptibility allele, possess non-NOD alleles at these loci (Table 3). Of the mutations within the *Il2* gene, the polyglutamine stretch is unlikely to be *Idd3* as both the PWK and SEG strains have polyglutamine stretches with lengths different from NOD (Table 3); the 4–amino acid insertion is also unlikely to be *Idd3* as it is absent in the PWK strain (Table 3). The serine/proline substitution at position 9 is also an unlikely candidate, given that the SEG strain has a serine at position 9, whereas NOD has a proline (Table 3). The only known allelic variant within the *Idd3* region remaining that is consistent with current data is the serine/proline substitution at position 6 of the mature IL-2 protein.

Analysis of the human *IL2* gene. Although linkage of IDDM to *IL2* has not been reported, it is a characteristic of polygenes that analysis of a marker in the actual candidate in

TABLE 3
Segregation analysis of polymorphisms within the 0.35-cM *Idd3* interval

Mouse strain	Is segregation observed at *Idd3* in cross with NOD?	Is NOD allele present at: *D3Nds55*?	*D3Mit239*?	*D3Nds36*?	Predicted amino acid sequence at *Il2* exon 1 x xxxx x	Is NOD allele present at: *D3Nds6*?	*D3Nds34*?	*D3Nds40*?
NOD		+	+	+	APTSSPTSSPTSSSTAEA(Q)$_8$ HLEQLLMDLQELLSRME	+	+	+
PWK	No*	–	–	–	APTSSPT - - - - SSSTAEA(Q)$_{19}$ HLEQLLMDLQELLSRME	–	–	–
SWR	No†	–	+	–	APTSSPTSSPTSSSTAEA(Q)$_8$ HLEQLLMDLQELLSRME	–	–	–
C57BL/6	Yes (3,4)	–	–	–	APTSSST - - - - SSSTAEA(Q)$_{12}$ HLEQLLMDLQELLSRME	–	–	–
NON	Yes (7)	+	+	–	APTSSST - - - - SSSTAEA(Q)$_{12}$ HLEQLLMDLQELLSRME	–	–	–
SEG	No (33)	–	–	–	APTSSPTSSSTSSSTAEA(Q)$_5$ HLEQLLMDLQELLSRME	–	–	–
ABH	No§	–	–	–	APTSSPTSSPTSSSTAEA(Q)$_8$ HLEQLLMDLQELLSRME	–	+	+

x, sites of coding mutations; +, NOD allele; –, non-NOD allele. *E. Melanitou, Pasteur Institute, Paris, France, personal communication. †E.H. Leiter, Jackson Laboratory, Bar Harbor, Maine, personal communication. §D. Baker, Institute of Opthalmology, London, U.K., personal communication.

larger numbers of families could reveal linkage. Moreover, intrafamilial association analysis is much more sensitive than affected sib pair analysis if the marker is in linkage disequilibrium with disease. Given this, we looked for evidence of linkage disequilibrium between a microsatellite linked to *IL2* and IDDM in 284 U.K. affected sib pairs. The *IL2* gene was mapped 11.9 cM distal to *D4S406* and 0.8 cM proximal to *D4S430*. There was no evidence of linkage disequilibrium between any of the alleles of the *IL2*-linked microsatellite and IDDM (data not shown). In addition, no evidence of linkage (186 sharing 1 allele identical by descent [IBD] versus 213 sharing 0 alleles IBD) was observed. Because the serine at position 6 is conserved between the two species, we sequenced exon 1 of the *IL2* gene in 103 individuals to determine if the same polymorphism exists in humans. Although polymorphisms have previously been reported (20,21) in exon 1 of the *IL2* gene, the only polymorphism we observed in 206 Caucasian and black chromosomes was a T to G substitution at nucleotide position 742. Of the 103 individuals sequenced, 21 were homozygous for the T allele, 57 were homozygous for the G allele, and 25 were heterozygous. The substitution was silent, occurring at position 3 of codon 38 of the *IL2* gene.

DISCUSSION

Identifying genes encoding susceptibility to polygenic traits such as IDDM is a major experimental challenge. A genome-wide scan in the NOD mouse (5,6) proved that the genes encoding diabetes—and, for that matter, any complex trait—could be mapped by linkage, setting the scene for similar studies in humans (22). However, unless very large numbers of families are available, such linkage studies will be unable to finely map loci to regions amenable to physical mapping (23). Although linkage disequilibrium mapping can be used in humans to more finely map loci (24), such an approach is not an option with the NOD mouse. Moreover, because *Idd* alleles have a dominant mode of inheritance coupled with low penetrance (1), the *Idd* loci cannot be mapped using standard outcrosses. Consequently, we used the approach of congenic mapping (3,4). In this study, we demonstrated that such an approach will allow the intervals containing *Idd* loci to be reduced to a size small enough to allow positional cloning and, as the gene map becomes more dense, positional candidate analysis (25).

Aod2, a locus encoding susceptibility to autoimmune ovarian dysgenesis (AOD), a disease with a Th-1 cell–mediated pathology similar to IDDM (26), has recently been mapped to proximal chromosome 3, with peak linkage occurring at *D3Mit182* (27), 3 cM distal to *Il2*. The potential colocalization of *Aod2* and *Idd3* (28) raises the interesting possibility that the same gene is involved with both autoimmune diseases. If this is indeed the case, it is likely that the gene encodes a protein involved in immune function. Of the genes mapped to the 0.35-cM interval containing *Idd3*, *Il2* is clearly an excellent candidate given its role as an immunomodulatory factor. Moreover, it has previously been shown that amino acid variations exist between the NOD and B6 forms of IL-2 (6,29). Despite the observed structural differences, no functional differences in T-cell proliferation assays between the two forms of IL-2 have been observed (29). It is, however, possible that a mutation such as the serine/threonine substitution at position 6 of the mature protein could affect the active half-life of the protein or its affinity for other forms of the IL-2 receptor (30), which would not be detected in crude proliferation assays.

Given this possibility, we more thoroughly examined all of the identified variants within and surrounding the *Il2* gene and the segregation of *Idd3* in crosses between NOD and a series of nondiabetic strains. The segregation analysis data we present provide preliminary evidence against all of the currently identified variants, except for the serine/proline substitution at position 6 of the mature form of IL-2. This finding, however, provides only circumstantial evidence for mapping *Idd3* to *Il2* because it relies on these assumptions: *1*) *Idd3* is a single genetic element, *2*) *Idd3* has one diabetes-susceptibility allele and one diabetes resistance allele, and *3*) when *Idd3* segregation is not observed, this is not due to the variable penetrance of *Idd3* but to the presence of the diabetes-susceptibility allele at *Idd3* in the diabetes-resistant strain.

As part of our segregation analysis of variants within *Idd3*, we also sequenced exon 1 of *Il2* in strains for which we do not yet have *Idd3* segregation data, such as 129/Sv, C3H, CBA, *Mus. castaneus*, DBA, ILI, A/J, ABL, and BALB/c (C.J.L., J.A.T., unpublished data). Among these strains, 129 have a previously unidentified serine/proline substitution at position 10 of the mature IL-2 protein (C.J.L., J.A.T., unpublished data). We are now carrying out segregation analyses at *Idd3* in 129 to assess whether or not this mutation can be excluded from *Idd3*. The only data inconsistent with *Il2* being *Idd3* come from a cross involving NOD and NZW (31). Preliminary data indicate that the *Il2* region of chromosome 3 segregates with susceptibility to insulitis in this cross. Because NOD and NZW have identical *Il2* genes, this, combined with the assumptions outline above, would argue against *Il2* exon 1 being responsible for insulitis in this cross. However, this work remains unconfirmed, and the number of progeny analyzed was extremely small. Sequence variation is also seen in the *Il2* genes of the two strains used in the AOD cross, A/J and B6, with A/J (which is the susceptible strain) having a sequence identical to NOD. This is consistent with *Il2* being *Aod2*.

Evidence of linkage to diabetes in other species would greatly strengthen the case for *Il2* encoding *Idd3*. However, no evidence of either linkage or linkage disequilibrium between *IL2* and IDDM in humans was observed in 284 United Kingdom affected sib pairs.

It is interesting to speculate how the serine/proline substitution might affect IL-2 function. It is known that the threonine residue at position 3 of the human form of IL-2 is glycosylated, and that this residue is important for the binding of IL-2 to the IL-2 receptor β molecule (32). This residue is contained within the motif PTSS, which is conserved between the human and mouse forms of IL-2. This motif is present once in the B6 form of IL-2; however, the serine/proline substitution in NOD mice leads to the duplication of this motif. Assuming that this threonine residue is also glycosylated in mouse, the duplication of the PTSS motif may lead to the NOD and B6 forms of IL-2 being differentially glycosylated. Differences in glycosylation could affect protein stability, receptor binding activity, or the amount of protein secreted.

To definitively determine whether the mutations within *Il2* exon 1 account for the activity of *Idd3*, we have embarked on the strategy of replacing the C57BL/6 form of exon 1 with the NOD form of exon 1 by homologous recombination in C57BL/6 ES cells. C57BL/6 mice generated from

these ES cells will be backcrossed to NOD to establish whether the exchange of *Il2* exon 1 has any effect on the frequency of disease. This congenic mouse gene-targeting approach will provide a powerful tool for testing the candidacy of not only NOD mouse mutations but also human mutations.

ACKNOWLEDGMENTS

This work was funded by the Wellcome Trust. C.J.L. is the recipient of a Wellcome Trust Prize Studentship, and J.A.T. is a Wellcome Trust Principal Research Fellow.

We would like to thank Karen Davis of the Molecular Cytogenetics Unit at the Wellcome Trust Centre for Human Genetics for technical assistance and performing the FISH analysis. We would also like to thank Drs. E. Melanitou, E. Leiter, and D. Baker for making data available prior to publication, and Dr. D. Beier for providing the *Anx-rs* primer sequences.

REFERENCES

1. Wicker LS, Todd JA, Peterson LB: Genetic control of autoimmune diabetes in the NOD mouse. *Annu Rev Immunol* 13:179–200, 1995
2. Ikegami H, Makino S, Yamato E, Kawaguchi Y, Ueda H, Sakamoto T, Takekawa K, Ogihara T: Identification of a new susceptibility locus for insulin-dependent diabetes mellitus by ancestral haplotype congenic mapping. *J Clin Invest* 96:1936–1942, 1995
3. Wicker LS, Todd JA, Prins J-B, Podolin PL, Renjilian RJ, Peterson LB: Resistance alleles at two non-major histocompatibility complex-linked insulin-dependent diabetes loci on chromosome 3, *Idd3* and *Idd10*, protect nonobese diabetic mice from diabetes. *J Exp Med* 180:1705–1713, 1994
4. Lord CJ, Bohlander SK, Hopes EA, Montague CT, Hill NJ, Prins J-B, Peterson LB, Wicker LS, Todd JA, Denny P: Mapping of the diabetes polygene *Idd3* on mouse chromosome 3 using novel congenic strains. *Mamm Genome* 6:563–570, 1995
5. Todd JA, Aitman TJ, Cornall RJ, Ghosh S, Hall JRS, Hearne CM, Knight AM, Love JM, McAleer MA, Prins J-B, Rodrigues N, Lathrop GM, Pressey A, DeLarato N, Peterson LB, Wicker LS: Genetic analysis of autoimmune type 1 diabetes mellitus in mice. *Nature* 351:542–547, 1991
6. Ghosh S, Palmer SM, Rodrigues NR, Cordell HJ, Hearne CM, Cornall R, Prins J-B, McShane P, Lathrop GM, Peterson LB, Wicker LS, Todd JA: Polygenic control of autoimmune diabetes in nonobese diabetic mice. *Nature Genet* 4:404–409, 1993
7. McAleer MA, Reifsnyder P, Palmer SM, Prochazka M, Love JM, Copeman JB, Powell EE, Rodrigues NR, Prins J-P, Serreze DV, DeLarato NH, Wicker LS, Peterson LB, Schork NJ, Todd JA, Leiter EH: Crosses of NOD mice with the related NON strain: a polygenic model for type 1 diabetes. *Diabetes* 44:1186–1195, 1995
8. Love JM, Knight AM, McAleer M, Todd JA: Towards construction of a high resolution map of the mouse genome using PCR-analyzed microsatellites. *Nucleic Acids Res* 18:4123–4130, 1990
9. Boyle AL, Feltquite DM, Dracopoli NC, Housman DE, Ward DC: Rapid physical mapping of cloned DNA on banded mouse chromosomes by fluorescence in situ hybridization. *Genomics* 12:106–115, 1992
10. Sambrook J, Fritsch EF, Maniatis T: *Molecular Cloning: A Laboratory Manual*. New York, Cold Spring Harbor Laboratory Press, 1989
11. Riley J, Butler R, Ogilvie D, Finniear R, Jenner D, Powell S, Anand R, Smith JC, Markham AF: A novel, rapid method for the isolation of terminal sequences from yeast artificial chromosome (YAC) clones. *Nucleic Acids Res* 18:2887–2890, 1990
12. Korn B, Sedlacek Z, Manca A, Kioschis P, Konecki D, Lehrach H, Poustka A: A strategy for the selection of transcribed sequences in the Xq28 region. *Hum Mol Genet* 1:235–242, 1992
13. Munroe DJ, Haas M, Bric E, Whitton T, Aburatani H, Hunter K, Ward D, Housman DE: IRE-Bubble PCR: a rapid method for efficient and representative amplification of human genomic DNA sequences from complex sources. *Genomics* 19:506–514, 1994
14. Bain SC, Todd JA, Barnett AH: The British Diabetic Association—Warren Repository. *Autoimmunity* 7:83–85, 1990
15. Epplen C, Frank G, Gomolka M, Nagy M, Nurnberg P, Epplen JT: Dinucleotide repeat polymorphism in the IL2 and IL5RA genes. *Hum Mol Genet* 3:679, 1994
16. Copeman JB, Cucca F, Hearne CM, Cornall RJ, Reed PW, RØnningen KS, Undlien DE, Nistico L, Buzzetti R, Tosi R, Pociot F, Nerup J, Cornélis F, Barnett AH, Bain SC, Todd JA: Linkage disequilibrium mapping of a type 1 diabetes susceptibility gene (*IDDM7*) to human chromosome 2q31-q33. *Nature Genet* 9:80–85, 1995
17. Dietrich WF, Miller J, Steen R, Merchant MA, Damron-Boles D, Husain Z, Dredg R, Daley MJ, Ingalls KA, O'Conner TJ, Evans CA, DeAngelis MM, Levinson DM, Kruglyak L, Goodman N, N.G. C, Jenkins NA, Hawkins TL, Stein L, Page DC, Lander ES: A comprehensive genetic map of the mouse genome. *Nature* 380:149–152, 1996
18. Francis F, Burgtorf C, Denny P, Cox R, Zehetner G, Todd J, Lehrach H: Construction and preliminary analysis of a C57BL/6 total genomic P1 library. In *9th International Workshop: Molecular Genetics of the Mouse*. Edinburgh, 1994
19. European Collaborative Interspecific Backcross (EUCIB): Towards high resolution maps of the mouse and human genomes—a facility for ordering markers to 0.1 cM resolution: European Backcross Collaborative Group. *Hum Mol Genet* 3:621–627, 1994
20. Nishino N, Obaru K, Maeda S, Shimada K, Onoue K: Organisation of the DNA regions flanking the human interleukin 2 gene. *Biomed Res* 6:197–205, 1985
21. Xu D, Wu Y, Chen J, Yu L, Zhong M, Hui Y, Qu H: Expression of human IL-2 from gene transferred mouse melanoma cells and its effect on the growth of mouse melanoma. *Chung-Hua Min Kuo Wei Sheng Wu Chi Mien I Hsueh Tsa Chih* 13:78–82, 1993
22. Davies JL, Kawaguchi Y, Bennett ST, Copeman JB, Cordell HJ, Pritchard LE, Reed PW, Gough SCL, Jenkins SC, Palmer SM, Balfour KM, Rowe B, Farrall M, Barnett AH, Bain SC, Todd JA: A genome-wide search for human type 1 diabetes susceptibility genes. *Nature* 371:130–136, 1994
23. Kruglyak L, Lander ES: High-resolution genetic mapping of complex traits. *Am J Hum Genet* 56:1212–1223, 1995
24. Todd JA, Farrall M: Panning for gold: genome-wide scanning for linkage in type 1 diabetes. *Hum Mol Genet* 5:1443–1448, 1996
25. Collins FS: Positional cloning moves from perditional to traditional. *Nature Genet* 9:347–350, 1995
26. Wardell BB, Michael SD, Tung KSK, Todd JA, Blankenhorn EP, McEntee K, Sudweeks JD, Hansen WK, Meeker ND, Griffith JS, Livingstone KD, Teuscher C: *Aod1*, the immunoregulatory locus controlling abrogation of tolerance in neonatal thymectomy-induced autoimmune ovarian dysgenesis, maps to mouse chromosome 16. *Proc Natl Acad Sci USA* 92:4758–4762, 1995
27. Teuscher C, Wardell BB, Lunceford JK, Michael SD, Tung KSK: *Aod2*, the locus controlling development of atrophy in neonatal thymectomy-induced autoimmune ovarian dysgenesis, is linked to *Il2*, *Fgfb*, and *Idd3*. *J Exp Med* 183:631–637, 1996
28. Vyse TJ, Todd JA: Genetic analysis of autoimmune disease. *Cell* 85:311–318, 1996
29. Chesnut K, She J-X, Cheng I, Muralidharan K, Wakeland EK: Characterizations of candidate genes for IDD susceptibility from the diabetes-prone NOD mouse strain. *Mamm Genome* 4:549–554, 1993
30. Wicker L, Wekerle H: Autoimmunity—editorial overview. *Curr Opin Immunol* 7:783–785, 1995
31. Funahashi M, Obata M, Shimpo K, Winter WE: Chromosome 3 GLUT2^{nod} polymorphisms are associated with insulitis in [(NOD × NZW) F1 × NOD] backcross mice. *Diabetes* 41:14A, 1992
32. Moreau J-L, Bossus M, De Groote D, Francois C, Jacques Y, Tartar A, Theze J: Characterization of a monoclonal antibody directed against the NH2 terminal area of interleukin-2 (IL-2) and inhibiting specifically the binding of IL-2 to IL-2 receptor beta chain. *Mol Immunol* 32:1047–1056, 1995
33. de Gouyon B, Melanitou E, Richard M, Requarth M, Hahn I, Guenet J, Demenais F, Julier C, Lathrop G, Boitard C, Avner P: Genetic analysis of diabetes and insulitis in an interspecific cross of the nonobese diabetic mouse with *Mus spretus*. *Proc Natl Acad Sci USA* 90:1877–1881, 1993